Cationic Self-Assembled Monolayers Composed of Gemini-Structured Dithiol on Gold: A New Concept for Molecular Recognition Because of the Distance between Adsorption Sites

Shinobu Yokokawa,[†,‡] Kaoru Tamada,*[,‡,§] Eisuke Ito,[‡] and Masahiko Hara*[,†,‡]

Department of Electronic Chemistry, Interdisciplinary Graduate School of Science and Engineering, Tokyo Institute of Technology, 4259 Nagatsuta-cho, Midori-ku, Yokohama, 226-8502, Japan, Local Spatio-Temporal Functions Laboratory, Frontier Research System, RIKEN (The Institute of Physical and Chemical Research), 2-1 Hirosawa, Wako-shi, Saitama, 351-0198, Japan, and Photonics Research Institute, National Institute of Advanced Industrial Science and Technology (AIST), 1-1-1 Higashi, Tsukuba, Ibaraki, 305-8565, Japan

Received: November 1, 2002; In Final Form: January 7, 2003

Cationic self-assembled monolayers (SAMs) composed of quaternary ammonium (QA) sulfur derivatives have been synthesized to control the distance between charged headgroups on gold substrates. Two molecules bearing resembling molecular structures, "gemini"-structured didodecyl dithiol (**HS-gQA-SH**) and didodecyl disulfide (**QA-SS-QA**), were utilized in this study, and the formation and structure of the SAMs were characterized by surface plasmon resonance spectroscopy (SPR), X-ray photoelectron spectroscopy (XPS), and Fourier transform infrared-reflection adsorption spectroscopy (FTIR−RAS). In the **HS-gQA-SH** SAM, the orientation and distance between QA groups are specified by the covalent bonding with ethylene spacer, while those of the **QA-SS-QA** SAM are determined by the electric repulsion between charged headgroups, that is, QA groups in the **QA-SS-QA** SAM are more randomly located, being more distant than with those in the **HS-gQA-SH** SAM. We found that L-tartaric acid, a probe molecule with two carboxyl groups having the distance of an ethylene unit, exhibits a strong affinity on the **HS-gQA-SH** SAM. In contrast, no specific binding was observed on the **QA-SS-QA** SAM. *These results imply the possibility to build up a molecular recognition system on surfaces because of the control of the distance between the charged headgroups by using the gemini-structured molecular design.*

1. Introduction

Self-assembled supramolecular structures in biological systems are constructed by molecular recognitions, where both the architecture and the function are often controlled by noncovalent bonding interactions,[1,2] such as hydrogen bonding and $\pi-\pi$ stacking as well as ionic interactions. The cell membranes made up of surfactants are one of the most sophisticated examples of such a natural supramolecular system, in which surfactants show interesting interfacial and bulk properties which tune the molecular structure. In the field of organic chemistry, the synthesis of new surfactants has also been attracting the attention of chemists for several years.[3] Recently, amphiphilic molecules with unique structures, "gemini" (dimeric) surfactants as a typical example,[4] have been synthesized to introduce structural diversity in these aggregates, such as rods, ribbons, helices, and tubes. The gemini surfactant contains two headgroups and two aliphatic chains, linked by a rigid or flexible spacer. An important feature of the gemini surfactants is that they show very low critical micellar concentrations (cmc) and superior surface-active properties compared to those of the corresponding monomeric ammoniums. Bis(quaternary ammonium)s with the structure of C_sH_{2s}-α,ω-$(Me_2N^+C_mH_{2m+1}Br^-)_2$, named *m*−*s*−*m*, are the molecules which have been most intensively studied in the gemini surfactant systems, in which the effects of spacer length,[5] added salts,[6] and the counterions[7] on the morphology and physical properties of self-assemblies have been investigated. Oda et al. reported transmission electron microscope (TEM) images of the gel formed by 16−2−16 gemini surfactant with L- or D-tartrate counterions in organic solvents (counterion-coupled gemini surfactants; cocogems[8]). They formed long entangled helical fibers, in which the degree of twist and the pitch of the ribbons can be tuned by the introduction of opposite-handed chiral counterions in various proportions.[9] It is of particular interest that the large scale of chirality in their supramolecular structure (helical or twisted ribbons) was induced by the molecular level of chirality introduced by chiral counterions (L- or D-tartrates). The cocogems system composed of two cetyltrimethylammonium ions and a single tartrate ($CTMA_2$-tartrate) was also investigated as an example of the gel formation from anisotropic molecules.[10] Polymerization of hydrophilic monomers (e.g., acrylamide) in the aqueous lyotropic phases has been studied as well, which resulted in highly ordered gels with a layerlike architecture between the submicrometer and micrometer length scale.

Self-assembled monolayers (SAMs) composed of organosulfur compounds on noble metals (e.g., gold and silver) have shown great promise as a means of controlling a two-dimensional (2D) chemical structure on a solid support.[11] A charged 2D surface as an analogue of 3D aggregates of ionized surfactants can easily be created by the self-assembling technique with thiol derivatives having ionized functional groups

* To whom correspondence should be addressed. Kaoru Tamada: e-mail: k-tamada@aist.go.jp; tel: +81-48-462-1111; fax: +81-48-462-4630. Masahiko Hara: e-mail: masahara@postman.riken.go.jp; tel: +81-298-61-6305; fax: +81-298-61-6303.

† Tokyo Institute of Technology.

‡ The Institute of Physical and Chemical Research.

§ National Institute of Advanced Industrial Science and Technology.

10.1021/jp027375m CCC: $25.00
Published on Web 03/20/2003

SCHEME 1: Molecular Structures of HS-gQA-SH and QA-SS-QA

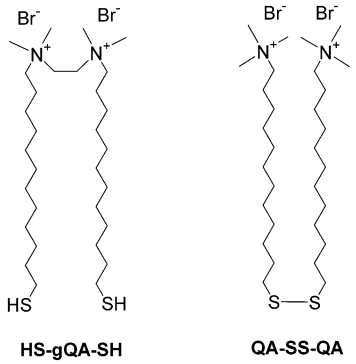

such as carboxylate and quaternary ammonium (QA).[12−14] Whitesides and co-workers fabricated the electrostatic SAMs having positive, negative, and both charged terminal groups. However, electric repulsion forces between charged groups prevent the formation of fully adsorbed SAMs, and the ellipsometric thickness of the SAMs estimated was much smaller than the molecular length. A significant influence of experimental conditions (temperature, solution concentration, polarity of the solvent, salt intensity, pH in aqueous solutions, and so on) is expected for such ionized systems; however, in their study, they did not optimize the preparation conditions of the SAMs to obtain the fully adsorbed SAMs.

In this paper, we combine both the interests concerning the cocogems and the functional SAMs and study cationic SAMs composed of QA sulfur derivative with gemini structure (**HS-gQA-SH**) on gold (Scheme 1, left). In the **HS-gQA-SH** SAM, the distance between QA groups is specified by the covalent connections with ethylene spacer. A didodecyl disulfide derivative (**QA-SS-QA**) is also synthesized and utilized in this study (Scheme 1, right) to draw a comparison with the property of **HS-gQA-SH** SAM. The formation and structure of the SAMs are characterized by surface plasmon resonance spectroscopy (SPR),[15] X-ray photoelectron spectroscopy (XPS), and Fourier transform infrared-reflection adsorption spectroscopy (FTIR−RAS). We also monitor the adsorption of L-tartaric acid, a probe molecule with two carboxyl groups having the distance of an ethylene unit, on **HS-gQA-SH** and **QA-SS-QA** SAMs, where the specific interactions between **HS-gQA-SH** and L-tartrate because of the distance between charged functional groups are expected. The SPR and XPS are utilized to confirm the adsorption of L-tartrate layers, while FTIR−RAS is utilized to determine the ionic state of two carboxyl groups on the surface.

2. Experimental Section

2.1. Materials. All chemicals were purchased from Kanto Chemical Co. Ltd. and used as received. Melting points of synthesized compounds were measured with an MP-500D melting-point apparatus (Yanaco Co. Ltd., Japan). ^{1}H NMR spectra were taken with JEOL α-400 (JEOL Co. Ltd., Japan) using tetramethylsilane (Merck) as an internal standard. Elemental analysis was performed with a Perkin-Elmer 240 (Perkin-Elmer Co. Ltd.).

Gemini-structured didodecyl dithiols (ethylenebis[(12-mercaptododecyl)dimethylammonium bromide], **HS-gQA-SH**), and didodecyl disulfide ((dithiodidodecylene)bis[trimethylammonium bromide], **QA-SS-QA**) were synthesized according to the methods in the literature.[14,16] The synthetic routes are shown in Scheme 2, in which the free thiol was obtained by hydrolysis of the thioacetate with hydrobromic acid without exchanging the counteranion.

*Thioacetic Acid S-(12-bromododecyl) Ester (**1**).* 1,12-dibromododecane (32.3 g, 100 mmol) and potassium thioacetate (2.86 g, 25.0 mmol) were dissolved in acetonitrile (300 mL) and the mixture was heated under reflux for 24 h. The reaction mixture was poured into water (500 mL) and extracted with ether (100 mL × 3). A combined organic layer was washed with water, dried over anhydrous magnesium sulfate, and evaporated to dryness. Flash chromatography using 95:5 hexane/ethyl acetate as eluant yielded **1** as a colorless oil (7.03 g, 87%). Anal. calcd for $C_{14}H_{27}BrOS$: C, 52.01; H, 8.42; Br, 24.71; S, 9.92%. Found: C, 51.95; H, 8.48; Br, 24.68; S, 9.90%. ^{1}H NMR (300 MHz, $CDCl_3$): δ (ppm) 1.15−1.65 (m, 18H, CH_2), 1.86 (qu, 2H, CH_2), 2.32 (s, 3H, CH_3CO), 2.86 (t, 2H, J = 7.2 Hz, CH_2S), 3.41 (t, 4H, J = 6.8 Hz, CH_2Br).

*1-Bromo-12-(12-bromododecyldisulfanyl)dodecane (**2**).* A solution of dry HCl in methanol was prepared by the addition of acetyl chloride (10 mL) to methanol (100 mL) at 0 °C. **1** (2.00 g, 6.19 mmol) was added and the solution was stirred at room temperature for 6 h. The reaction mixture was poured into water (100 mL) and extracted with ether (40 mL × 3). A combined organic layer was washed with water, dried over

SCHEME 2: Synthetic Route of HS-gQA-SH and QA-SS-QA

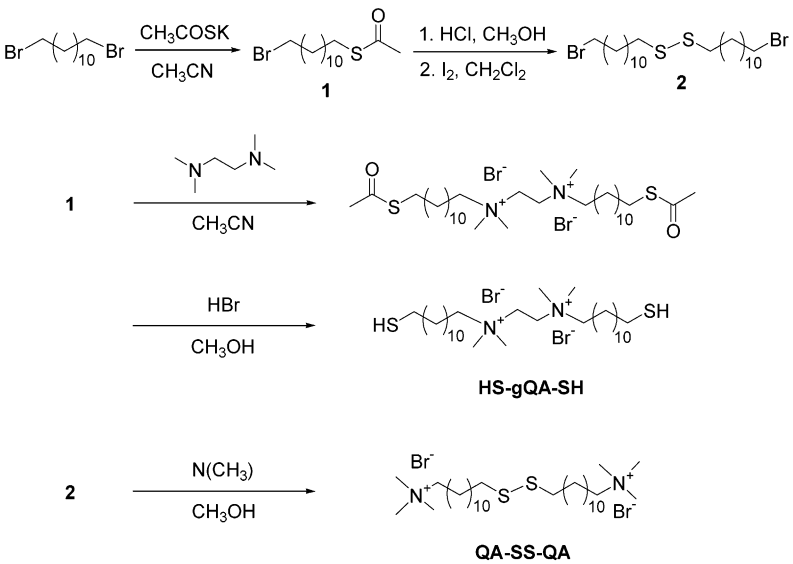

anhydrous magnesium sulfate, and evaporated to dryness. A solution of the residue in dichloromethane (20 mL) was titrated with a 0.1 M dichloromethane solution of I_2 until a yellow color persisted. The reaction mixture was poured into water (100 mL) and extracted with ether (30 mL × 3). A combined organic layer was washed with water, dried over anhydrous magnesium sulfate, and then evaporated under reduced pressure. The residue was recrystallized from hexane to yield **2** as a white solid (1.60 g, 92%), mp 50−51 °C. Anal. calcd for $C_{24}H_{48}Br_2S_2$: C, 52.42; H, 8.63; Br, 28.51; S, 11.44%. Found: C, 52.47; H, 8.63; Br, 24.41; S, 11.49%. ^{1}H NMR (300 MHz, $CDCl_3$): δ (ppm) 1.20−1.73 (m, 36H, CH_2), 1.85 (qu, 4H, J = 7.1 Hz, CH_2), 2.68 (t, 4H, J = 7.3 Hz, CH_2S), 3.41 (t, 4H, J = 6.9 Hz, CH_2Br).

*Ethylenebis[(12-mercaptododecyl)dimethylammonium bromide] (**HS-gQA-SH**).* The compound **1** (4.0 g, 12.4 mmol) and tetramethylethylene-diamine (TMEDA) (0.72 g, 6.2 mmol) were dissolved in acetonitrile (50 mL) and heated at 50 °C for 48 h. The reaction solution was evaporated under reduced pressure and was recrystallized from acetone to give a white solid. To a solution of the white solid in methanol (100 mL), 48% hydrobromic acid (0.5 mL) was added and the solution was stirred at room temperature for 4 h. The reaction solution was evaporated under reduced pressure and was recrystallized from acetone/methanol (98:2) to yield **HS-gQA-SH** as a white solid (1.77 g, 42%). Anal. calcd for $C_{30}H_{66}Br_2N_2S_2$: C, 53.08; H, 9.80; Br, 23.54; N, 4.13; S, 9.45%. Found: C, 52.95; H, 9.85; Br, 23.40; N, 4.12; S, 9.45%. ^{1}H NMR (300 MHz, DMSO): δ (ppm) 1.20−1.35 (m, 32H, CH_2), 1.54−1.70 (m, 8H, CH_2), 2.46 (q, 4H, J = 7.3 Hz, CH_2SH), 3.13 (s, 12H, CH_3N^+), 3.35−3.42 (m, 4H, CH_2N^+), 3.88 (s, 4H, N^+(CH_2)$_2N^+$).

*(Dithiodidodecylene)bis[trimethylammonium bromide] (**QA-SS-QA**).* The compound **2** (1.0 g, 1.78 mmol) was dissolved in trimethylamine methanol solution (50 mL, 25 w/w %, purchased from Sigma Co. Ltd) and was stirred at room temperature for 48 h. The reaction solution was evaporated under reduced pressure and was recrystallized from acetone to yield **QA-SS-QA** as a white solid (1.10 g, 91%). Anal. calcd for $C_{30}H_{66}Br_2N_2S_2$: C, 53.08; H, 9.80; Br, 23.54; N, 4.13; S, 9.45%. Found: C, 53.02; H, 9.83; Br, 23.51; N, 4.13; S, 9.49%. ^{1}H NMR (300 MHz, DMSO): δ (ppm) 1.19−1.35 (m, 32H, CH_2), 1.54−1.71 (m, 8H, CH_2), 2.68 (t, 4H, J = 7.2 Hz, CH_2S), 3.03 (s, 18H, CH_3N^+), 3.25 (t, 4H, J = 8.4 Hz, CH_2N^+).

2.2. Gold Substrates and Monolayer Preparation. The gold (∼50 nm) for SPR measurement was deposited on high refractive index glass slides (LaSFN9, 25 × 35 mm) by thermal deposition in a vacuum chamber at ∼1 × 10^{-5} Torr (BIEMTRON Co. Ltd., Japan). The substrates for the FTIR−RAS measurement were prepared by deposition of 200-nm-thick gold on the glass slides with 5-nm-thick chromium adhesion layers by using the same vacuum chamber as that for SPR measurement. The bare Au/Cr substrate for background measurement was deposited at the same time to minimize the experimental error arising from thickness and roughness of gold, which was cleaned just before use with chloroform to remove surface contamination.

Au(111)/mica substrates for XPS measurement were prepared by the epitaxial growth of a 100∼150-nm gold film onto freshly cleaved mica in a laboratory built vacuum chamber. Gold was thermally deposited on a mica surface prebaked at 300 °C for 24 h, which is measured on the back surface of the substrate holder. Deposition was carried out and the substrate temperature was controlled at 300 °C during deposition at a pressure 10^{-7} ∼ 10^{-8} Torr. After deposition, the substrate was annealed at 470 °C for 6 h.

For SAM formations, **HS-gQA-SH** and **QA-SS-QA** were dissolved in methanol at various concentrations (0.01 mM and 0.1 mM). The SAMs for SPR measurements were prepared in situ by injection of the solutions with sulfur compounds into the liquid cell. The SAMs for XPS and FTIR−RAS measurements were prepared ex situ by immersing gold substrates in the methanol solutions for 6 h at room temperature, and at the designated times, the substrates were quickly removed from the solution and immediately rinsed with absolute methanol and dried in a stream of N_2. The adsorption of L-tartaric acid (99.5%) on the SAMs was conducted with a 1.0 mM methanol solution by 6 h immersion. The XPS and FTIR−RAS measurements were performed within 24 h after preparation of the SAMs. The detailed experimental conditions are described in the following paragraphs with the experimental data.

2.3. Characterization. Surface Plasmon Resonance Spectroscopy (SPR).[17] The SPR measurement setup was based on the configuration introduced by Kretschmann and Raether.[18] The details of the experimental setup have been described elsewhere.[19] A 45° prism with high refractive index glass (LaSFN9, n = 1.84 at a λ = 632.8 nm) was used, and all the liquid cells (internal volume, ∼3 mL) and the tubes were made of Teflon, which is resistant to organic solvents. The temperature of the cell was kept at 20 °C during the SPR measurement by a thermostat. A p-polarized laser beam (He−Ne, λ = 632.8 nm, maximum power 5 mW) was used as the light source, which was mechanically chopped in conjunction with a lock-in amplifier before entry into the prism. The intensity of the beam reflected at the gold interface was detected by a photodiode detector and recorded as a function of the incidence angle for "angular-scan" measurements or as a function of time at a fixed angle of incidence for "kinetics-scan" measurements.

The thickness and complex refractive index of the gold layer were determined by curve fitting of the SPR data (angular scan) in absolute methanol.[18,20] A 5-mL solution with sulfur compounds was injected into the cell for SAM formation, and the adsorption process was monitored via the change of reflectivity by the kinetics-scan measurement (incidence angle 55°). The SPR measurements were carried out in various polar solvents (methanol, ethanol, and water) to estimate both the thickness and the refractive indices of the SAMs.[21] During this procedure, one solvent was successively replaced by another solvent, and the measurements with methanol were performed several times intermittently to confirm that there is no damage or contamination on the SAM because of exposure to the new solvents: methanol (first) → ethanol → methanol (second) → air → methanol (third).

X-ray Photoelectron Spectroscopy (XPS). XPS measurements were carried out with the ESCALAB 250 system (Thermo VG Scientific Co. Ltd., U.K.). The 150 V monochromatized Al K_α line was used as an excitation source. The binding energy in XPS spectra was calibrated with the Au 4f7/2 peak at 83.9 eV. The energy positions and intensities of S 2p and C 1s peaks were determined by curve-fitting analysis with Voigt functions. Since one chemical state of S has two splitting peaks due to the spin−orbital interaction (S 2p3/2 and S 2p1/2), we need to take into account this splitting of binding energy (∼1.2 eV) and the ratio of the peak intensity (S 2p3/2:S 2p1/2 = 2:1) for the data analysis.

Fourier Transform Infrared Spectroscopy (FTIR). Infrared spectra of the bulk materials were taken by the single-reflection ATR-powder method (Thunderdome Module), while those of the SAMs were taken in the reflection mode (incidence angle: 80° to the surface normal) using a p-polarized beam with

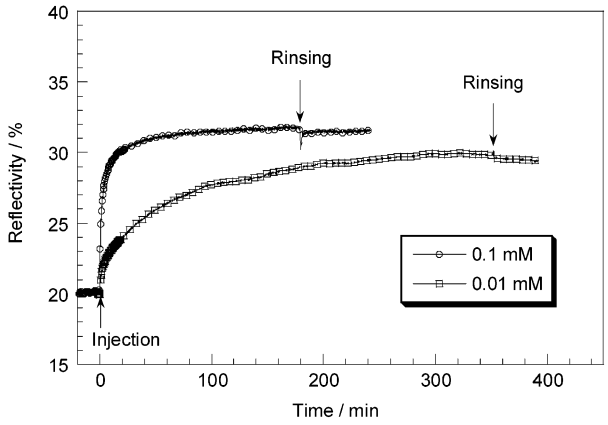

Figure 1. Adsorption kinetics of **HS-gQA-SH** on gold from the methanol solutions with various thiol concentrations, 0.1 mM and 0.01 mM.

SCHEME 3: Conformational Model of HS-gQA-SH Adsorbed on Gold Surface

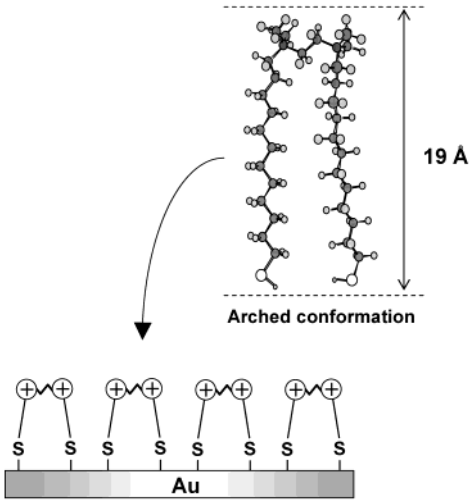

NEXUS 670 FT-IR (Thermo Nicolet Co. Ltd.). The spectrometer was purged with dry nitrogen, and a liquid-nitrogen-cooled mercury−cadmium-telluride (MCT) detector was used for the reflection measurements. The spectra were recorded at a 4 cm^{-1} resolution with 1024 scans in the 800∼4000 cm^{-1} region. The experimental error to determine the peak position was estimated to be approximately ± 1 cm^{-1}.

3. Results and Discussion

3.1. Optimization of Preparation Conditions for HS-gQA-SH on Gold. Since **HS-gQA-SH** has two SH groups, two kinds of adsorption should be considered; one is the adsorption by one SH group ("stretched" conformation), the other is that by both SH groups ("arched" conformation). We varied the concentration of the methanol solution with **HS-gQA-SH** and monitored the film formation process on gold with SPR. The SPR data shown in Figure 1 in 0.01 mM and 0.1 mM demonstrate different adsorption kinetics and the final SAM thickness of **HS-gQA-SH** because of the concentration of the solutions. The thickness of the **HS-gQA-SH** SAMs was estimated from the SPR angular scan data where the refractive index $n = 1.50$ is utilized for the calculation of 16 Å (0.01 mM) and 26 Å (0.1 mM). As schematically shown in Scheme 3, the thickness of the SAM with the "arched" conformation is estimated to be 23 Å, which is the molecular height from the molecular modeling (19 Å) plus the thickness of the thiolate layer (4 Å[21,22]), and 16 Å in 0.01 mM indicates that the growth of the SAM is almost saturated under a less dense condition. Since "stretched" conformation would have at least a thickness of 38 Å thickness, the 0.1 mM methanol solution is also considered to provide the "arched" conformation as suggested from the following XPS measurements.

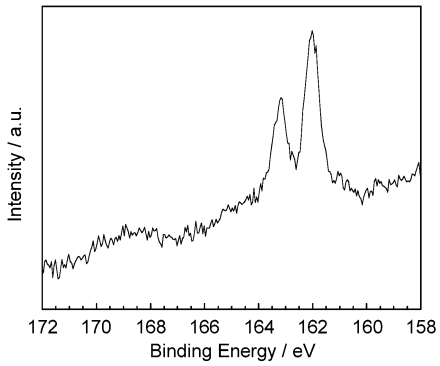

Figure 2. High-resolution S(2p) XPS spectrum of **HS-gQA-SH** SAM on Au(111) formed from 0.1 mM methanol solution.

Figure 2 shows the binding condition of sulfur in the SAM which is prepared from 0.1 mM methanol solution and characterized by high-resolution XPS. The S2p peaks appeared as doublets at 163.2 eV (2p1/2) and 162 eV (2p3/2); these are assigned as sulfur atoms bound to gold.[23] That is to say, both of the SH groups in **HS-gQA-SH** are chemisorbed on Au(111) by forming an "arched" molecular conformation on gold (Scheme 3). In the higher concentration of the methanol solution than 0.1 mM, the S2p peaks tend to exhibit additional shoulders at the higher binding energy, suggesting the existence of "unbound" sulfur in the SAM,[23] that is, in high dithiol concentration; some of the **HS-gQA-SH** molecules adsorb on gold by one SH group forming a "stretched" molecular conformation.

On the basis of the results obtained with both SPR and XPS, we choose the solution concentration of 0.1 mM as a standard condition for the SAM preparation to keep the surface density of the molecules reasonably high but to still form the "arched" molecular conformation with both the SH groups reacting with gold. We also confirmed the influence of solvents utilized for the SAM formation, where methanol was found to give more stable and reproducible SAMs than the other polar solvents (water or ethanol).

3.2. Characterization of HS-gQA-SH and QA-SS-QA SAMs with SPR and FTIR−RAS. In Figure 3, we compared the adsorption kinetics of **HS-gQA-SH** on gold with that of **QA-SS-QA** (both are the adsorption from 0.1 mM methanol solutions). Both SAMs are stable against rinsing with absolute methanol as shown in Figure 3 and also with absolute ethanol and water.

The thickness values of the **HS-gQA-SH** and **QA-SS-QA** SAMs estimated from the SPR angular scan data are listed in Table 1 along with the data taken from references. Holmlin and co-workers have studied a similar type of QA SAM composed of *N*,*N*,*N*-trimethyl(11-mercaptoundecyl)ammonium chloride, $HS(CH_2)_{11}N^+(CH_3)_3Cl^-$, and reported the thickness of the SAM as 13 ± 1 Å with $n = 1.45$.[14] This thickness value was quite small compared with that of alkanethiol SAMs with a similar carbon number (e.g., the ellipsometric thickness of dodecanethiol SAM is estimated to be 21 ± 3 Å with $n = 1.45$ in air). First, we calculated the film thickness with $n = 1.45$ to perform a direct comparison with references values. As summarized in

TABLE 1: Thickness Values of HS-gQA-SH and QA-SS-QA SAMs Estimated from SPR Angular Scan Data along with the Thickness Data from the References

sulfur compound	SAM preparation condition (solvent/concentration/immersion time)	SAM thickness (Å)	comments
HS-gQA-SH	MeOH/0.1 mM/3 h	34 ± 3^a $(26 \pm 2)^c$	this work
QA-SS-QA	MeOH/0.1 mM/3 h	26 ± 3^a $(26 \pm 3)^c$	this work
$(CH_3)_3N^+(CH_2)_{11}SH \cdot Cl^-$	EtOH/1 mM/~24 h	13 ± 1^b	ellipsometry[d]
$CH_3(CH_2)_{11}SH$	EtOH/0.1−5 mM/2−3 days	21 ± 3^b	ellipsometry[e]

[a] The thickness is estimated with $n = 1.45$ in methanol. [b] The thickness is estimated with $n = 1.45$ in air. [c] The thickness is estimated by a contrast variation SPR technique (Figure 4). The utilized refractive index for the calculation: **HS-gQA-SH**; $n = 1.50 \pm 0.02$, **QA-SS-QA**; $n = 1.46 \pm 0.01$. [d] Reference 14. [e] Reference 22.

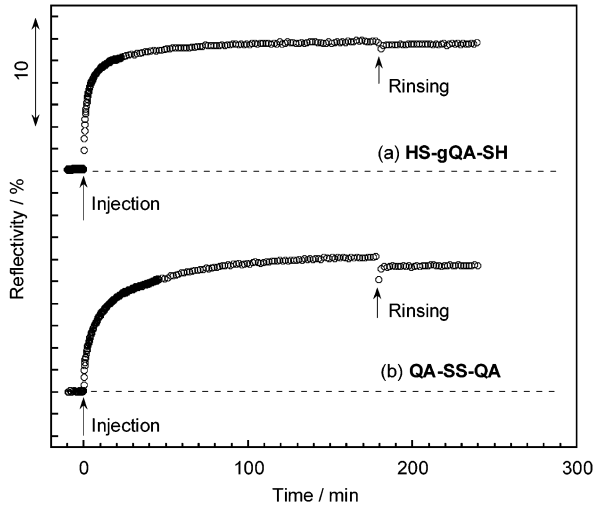

Figure 3. Adsorption kinetics of **HS-gQA-SH** (a) and **QA-SS-QA** (b) on gold from 0.1 mM methanol solutions.

Table 1, **HS-gQA-SH** and **QA-SS-QA** SAMs in our study are much thicker than the QA SAM reported by Holmlin et al.

We executed a more reliable analysis for the determination of the SAM thickness by a contrast variation SPR technique, that is, the determination of both the refractive index (n) and the thickness (d) of the SAM from SPR data taken in various solvents (in media with different refractive indices). Figure 4 shows the simulation results of n and d estimated from the SPR peak shift by an angular scan in methanol, ethanol, and air. If there is no solvent effect, such as swelling or adsorption of contaminants, the three simulation data must have one intersection point which indicates the "real" n and d of the SAM.[24] As shown in Figure 4, though there is a slight influence of swelling by solvents, the refractive index and the thickness of **HS-gQA-SH** SAM are estimated to be about $n = 1.50 \pm 0.02$ and $d = 26.0 \pm 0.3$ Å, respectively. On the other hand, for **QA-SS-QA** SAM, the refractive index and the thickness were estimated with $n = 1.46 \pm 0.01$ and $d = 25.7 \pm 0.2$ Å, respectively. These data suggest that the density of **HS-gQA-SH** SAMs is much higher than that of **QA-SS-QA** SAM, while they have almost equivalent thickness. In any case, the refractive indices obtained ($n = 1.50$ for the **HS-gQA-SH** SAM, $n = 1.46$ for the **QA-SS-QA** SAM) are quite reasonable for the thiol derivative SAMs on gold, and the thicknesses obtained ($d =$ 26 for both the SAMs) show good agreement with the thickness estimated from the extended molecular conformation as an analogue of alkanethiol SAMs. In particular, the "arched" conformation for **HS-gQA-SH** SAM is clearly confirmed by this thickness value.

The FTIR−RAS spectra of **HS-gQA-SH** and **QA-SS-QA** SAMs are shown in Figure 5. In both cases, the methylene stretching vibrations at 2924 and 2856 cm^{-1} indicate a slightly

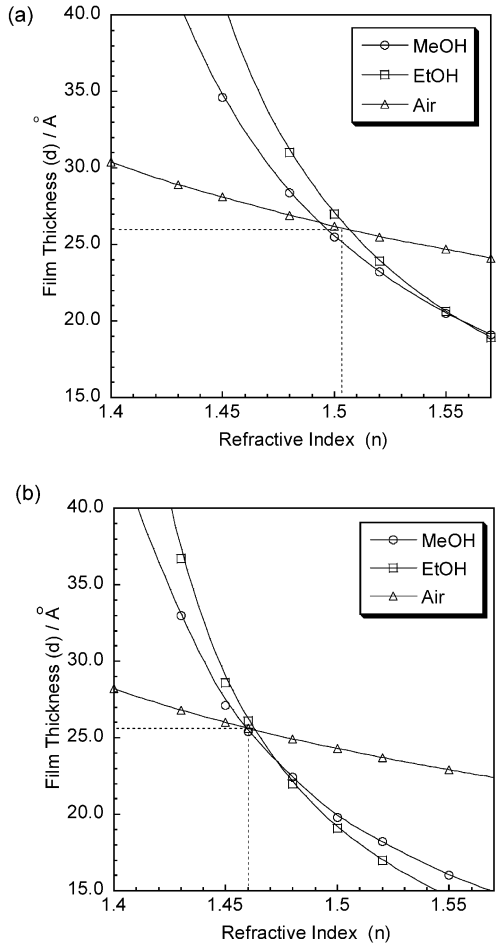

Figure 4. Film thickness (d) versus the refractive index (n) determined by a contrast variation SPR technique for **HS-gQA-SH** SAM (a) and **QA-SS-QA** SAM (b) formed from 0.1 mM methanol solution.

disordered packing of long alkyl spacer groups.[25] The intensities of these peaks are higher in the **HS-gQA-SH** SAM than those of the **QA-SS-QA** SAM, suggesting that the density of **HS-gQA-SH** SAM is higher than that of **QA-SS-QA** SAM, which is consistent with our SPR result. The peaks originating from QA groups, about 1400 ~ 1500 cm^{-1}, are not sufficiently clear to extend further discussions for the molecular confirmations.

3.3. Selective Adsorption of L-Tartaric Acid on the SAM Surface. We investigated the adsorption of L-tartaric acid on both the **HS-gQA-SH** and **QA-SS-QA** SAMs by in situ SPR measurements, and the results are shown in Figure 6. In this experiment, L-tartaric acid 1.0 mM methanol solution was injected into the SPR liquid cells, and after adsorption for 6 h, the surfaces were rinsed by absolute methanol. As shown in Figure 6, L-tartaric acid was adsorbed on both the **HS-gQA-SH** and **QA-SS-QA** SAMs, while it formed a much thicker layer

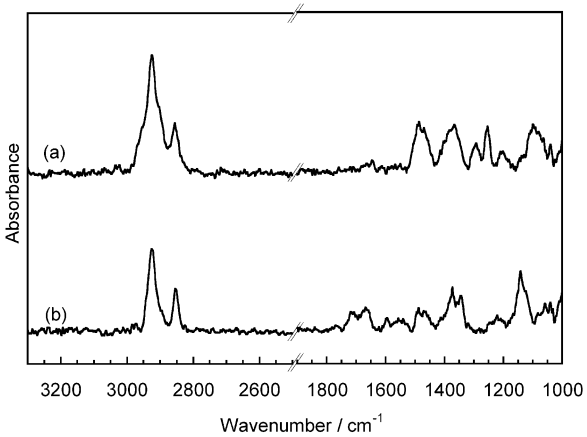

Figure 5. FTIR−RAS spectra of **HS-gQA-SH** SAM (a) and **QA-SS-QA** SAM (b) prepared by 8 h immersion in 0.1 mM methanol solution.

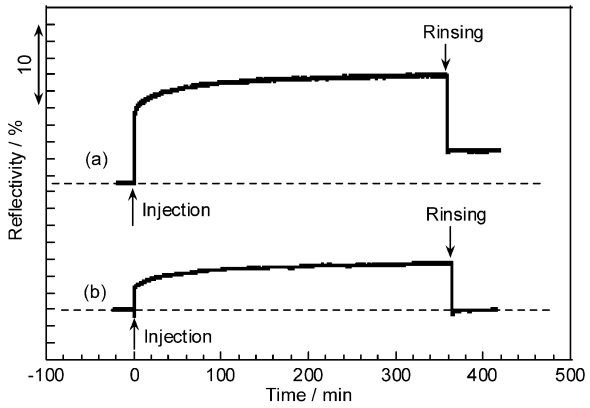

Figure 6. Adsorption of L-tartaric acid from 1.0 mM methanol solution on **HS-gQA-SH** SAM (a) and **QA-SS-QA** SAM (b). Both the SAMs are prepared by 6 h immersion in 0.1 mM methanol solutions.

on the **HS-gQA-SH** SAM. The adsorbed L-tartaric acid layer has quite a different response to the rinsing procedure; the layer could remain on the **HS-gQA-SH** SAMs even after rinsing (Figure 6a), however, that on **QA-SS-QA** SAM was almost completely rinsed out by the same rinsing procedure (Figure 6b). In fact, the thickness of the L-tartaric acid layer was varied because of the condition of the **HS-gQA-SH** and **QA-SS-QA** SAM layers determined by the film formation process (e.g., the solution concentration, the reaction time, and solvent);[26] however, a stable and thick adsorption layer was observed only on the **HS-gQA-SH** SAM. *The concentration of* L*-tartaric acid in solution did not affect the thickness of the* L*-tartaric acid layer but did affect the adsorption kinetics.*[27]

Next, we estimated the thickness of adsorbed L-tartaric acid layer from the SPR angular scan data, with the refractive index $n = 1.5$, which is the value for D-tartaric acid bulk crystals.[28] The results are listed in Table 2. The thickness of the L-tartaric acid layer on the **HS-gQA-SH** SAM was estimated to be 34 Å before rinsing and 7 Å after rinsing. By MM2 calculation, the height of L-tartaric acid layers anchored on the surface with both COOH groups is calculated as approximately 6 Å. Thus, the formation of L-tartaric acid multilayers before rinsing and that of monomolecular films after rinsing is suggested on the **HS-gQA-SH** SAM. On the other hand, for the **QA-SS-QA** SAM, L-tartaric acid could form multilayers on the SAM (layer thickness, 15 Å); however, all of the molecules were desorbed by rinsing, as already suggested by the kinetics data.

These surfaces are characterized by XPS. The relative peak intensities of carbon (C1s) and oxygen (O1s) against gold (Au4f)

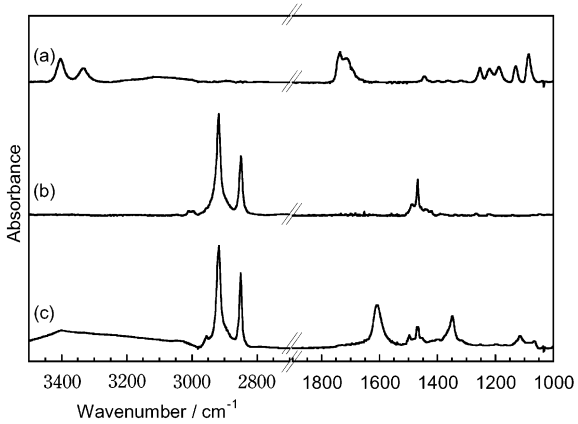

Figure 7. FTIR−ATR spectra with powders of neutral L-tartaric acid (a), **HS-gQA-SH** (b), and the ionic complex composed of these two molecules synthesized in solution, (**HS-gQA-SH**+Tartrate) (c).

TABLE 2: Thickness of Adsorbed L-Tartaric Acid Layer on HS-gQA-SH and QA-SS-QA SAMs Before and After Rinsing with Absolute Methanol

	thickness L-tartaric acid layer (Å)[a]	
SAM	before rinsing	after rinsing
HS-gQA-SH	34 ± 2	7 ± 2
QA-SS-QA	15 ± 3	1 ± 2

[a] The thickness of L-tartaric acid layer is estimated on the basis of the refractive index of D-tartaric acid bulk crystals, $n = 1.50$. See ref 27.

are determined on **HS-gQA-SH** and **QA-SS-QA** SAMs before and after adsorption of L-tartaric acid. Both SAMs and L-tartaric acid layers are prepared in the same way as those in Figure 3 and Figure 6, and the XPS data are taken only after rinsing with absolute methanol. *Relative peak intensities of C1s and O1s against Au4f were changed from 1.1 to 1.7 (C1s/ Au4f) and from 0.14 to 0.32 (O1s/Au4f), respectively, after adsorption of* L*-tartaric acid on the HS-gQA-SH SAM. On the other hand, those on the QA-SS-QA SAM were changed from 0.92 to 0.89 (C1s/Au4f) and from 0.23 to 0.29 (O1s/Au4f), respectively.* Pronounced increases of carbon and oxygen elements by adsorption of L-tartaric acid were found on the **HS-gQA-SH** SAM while no significant change was detected on the **QA-SS-QA** SAM. This result evidentially proves a selective adsorption of the L-tartaric acid onto the **HS-gQA-SH** SAM, in good agreement with the SPR data. The difference for adsorption of L-tartaric acids on these SAMs can be interpreted by the different orientations and distances between QA groups on each SAM as derived from their chemical structures. The details are discussed in the following section.

3.4. Adsorption Mechanism of Tartaric Acid on the Cationic SAMs. L-tartaric acid is considered to have at least three different ionized conditions: the neutral bi-acid form, the monotartrate by deprotonation of one of the carboxylic acid groups, and the bitartrate by deprotonation of both acid groups. We characterized the IR spectra of L-tartaric acid on the SAMs to confirm the ionized states of carboxylic acid groups because of the formation of an ion complex with QA groups on the surface.

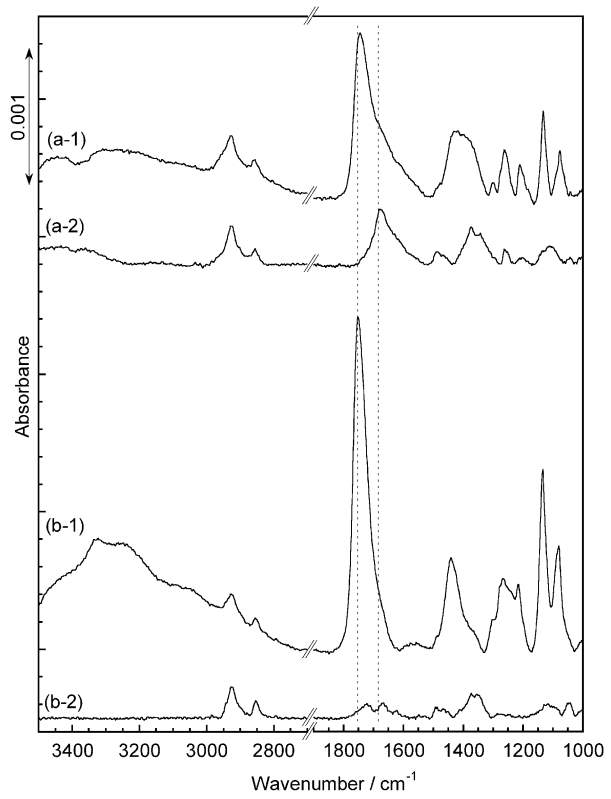

Figure 8. FTIR−RAS spectra of L-tartaric acid adsorbed on **HS-gQA-SH** (before rinsing: a-1, after rinsing: a-2) and on **QA-SS-QA** (before rinsing: b-1, after rinsing: b-2).

In Figure 7, we present FTIR−ATR spectra with powders of neutral L-**tartaric acid (a), HS-gQA-SH** (b), and the ionic complex of these two molecules (**HS-gQA-SH** + Tartrate) (c) synthesized in solution. *The band positions and their assignments are listed in Support Information.* For the neutral L-tartaric acid, the ν(C═O) and ν(C−O) vibrations appear at ∼1750 and 1380 cm^{-1}, respectively,[29] while the ν_{asym}(COO) and ν_s(COO) vibrations originated from deprotonated molecules appear at ∼1600 and 1400 cm^{-1}, respectively. Since no vibration modes from the cationic SAMs are overlapped in this frequency region except for a few peaks at 1400∼1500 cm^{-1}, we could detect the main vibration band from L-tartaric acid (1736, 1446 cm^{-2}) without interruption by the signal from the cationic SAMs.[30−32]

Figure 8 shows FTIR−RAS spectra of L-**tartaric acid on the HS-gQA-SH** and **QA-SS-QA** SAMs before (a-1, b-1) and after (a-2, b-2) rinsing, where the surfaces are prepared by the same condition as those for SPR measurements in Figure 3 and Figure 6. *The band positions and their assignments are listed in Support Information.* Before rinsing, the peak from L-tartaric acid adsorbed on the **HS-gQA-SH** SAM appeared at 1745 cm^{-1} at the position of ν(C═O) vibration together with the shoulder peak corresponding to ν_{asym}(COO). The data suggest both neutral and deprotonated carboxylic acid groups exist in the tartrate layer, that is, the existence of physisorbed L-tartaric acid molecules. After rinsing, only the peak corresponding to ν_{asym}-(COO) vibration is observed at 1678 cm^{-1}, indicating that only bitartrate molecules (both acid groups are deprotonated) remain on the surface. For the L-tartaric acid adsorbed on the **QA-SS-QA** SAM, a strong peak appeared at 1745 cm^{-1} at the position of ν(C═O) vibration before rinsing; however, only small doublet peaks at 1710 and 1667 cm^{-1} remained after rinsing. The data suggest the existence of a small amount of monotartrate on the surface resulting from deprotonation of one of the carboxylic acid groups, though the amount of adsorbed molecules is negligibly small.

On the basis of the SPR, XPS, and IR data, we propose the model for the adsorption mechanism of the L-tartaric acid on

SCHEME 4: Schematic Illustrations of Adsorption Mechanisms of L-Tartaric Acids on HS-gQA-SH and QA-SS-QA SAMs

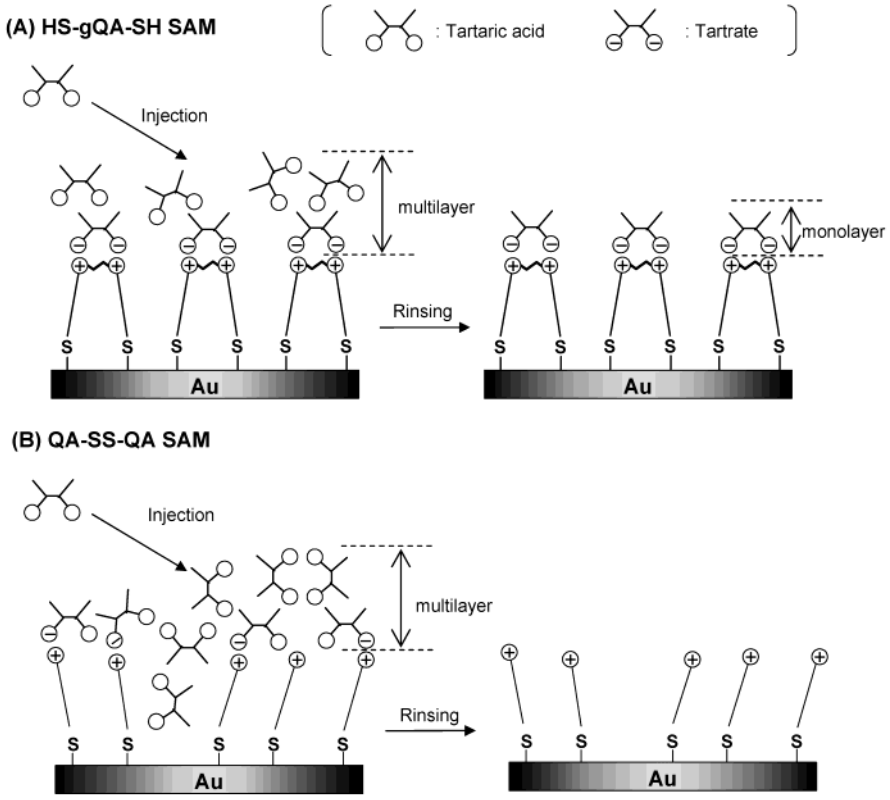

each SAM as drawn in Scheme 4. L-tartaric acids are adsorbed on the **HS-gQA-SH** SAM by the ionic interaction with two carboxylate (deprotonated carboxylic acid) groups, which results in L-tartrate being stable and resistant to the rinsing procedure. On the other hand, L-tartaric acids can anchor on the **QA-SS-QA** SAM only by one of the two carboxylic acid groups, and these weakly anchoring L-tartaric acids are desorbed by the rinsing procedure. In other words, the deprotonation of both of the carboxylic acids to carboxylates can be achieved only on the **HS-gQA-SH** SAM.

The difference between the **HS-gQA-SH** and **QA-SS-QA** SAMs is the distance and orientation of the charged headgroups. In the **HS-gQA-SH** SAM, the distance between QA groups is specified by the covalent bonding with ethylene spacer, while that of the **QA-SS-QA** SAM is spontaneously determined by the electrostatic repulsion between charged headgroups, that is, QA groups in the **QA-SS-QA** SAM must be more randomly located, being more distant than those in the **HS-gQA-SH** SAM. Two carboxyl groups in L-tartaric acid have the distance of an ethylene unit in the same way as the QA groups in the **HS-gQA-SH** SAM, which might be the origin of a strong affinity of L-tartrates on the **HS-gQA-SH** SAM. In contrast, no specific binding of L-tartaric acid was observed on the **QA-SS-QA** SAM, probably because of a "mismatching" of the distance and orientation between the functional groups. These results represent the possibility of building up highly selective molecular recognition systems on surfaces by the use of the gemini-structured synthetic molecules, that is, by controlling the distance of charged headgroups on the surface because of the specific molecular design.

4. Conclusion

The properties of **HS-gQA-SH** and **QA-SS-QA** SAMs on gold, particularly the selective adsorption of L-tartaric acid on the SAMs, were characterized by using SPR, XPS, and FTIR techniques. The covalent bonding between cationic headgroups (QA) in **HS-gQA-SH** resulted in the higher density of the SAM compared with that of **QA-SS-QA** SAM. The strong affinity between the gemini surfactants and L-tartaric acids can be interpreted by the matching of the lengths between the charged functional groups controlled by ethylene spacer units. Specifically framed functionality on the surface introduced by a gemini structure opens the door to a new concept for molecular recognition with the molecularly controlled distance and orientation of two-dimensional adsorption sites.

Acknowledgment. We thank Dr. R. Oda and Dr. I. Huc in the Institut Européen de Chimie et Biologie, Bordeaux, France, for fruitful discussions. We are grateful to Dr. H. Akiyama and Dr. J. Nagasawa in AIST for their help concerning the thiol synthesis. S. Yokokawa thanks the JRA fellowship of RIKEN.

Supporting Information Available: Vibration bands in FTIR-ATR spectra with powders of neutral L-tartaric acid (a), **HS-gQA-SH** (b), and the ionic complex composed of these two molecules synthesized in solution, (**HS-gQA-SH**+Tartrate) (c), and vibration bands in FTIR-RAS spectra of the L-tartaric acid adsorbed on **HS-gQA-SH** and on **QA-SS-QA** SAMs. This material is available free of charge via the Internet at http://pubs.acs.org.

References and Notes

(1) Stryer, L. *Biochemistry*; W. H. Freeman: New York, 1988.

(2) Lehn, J.-M. *Supramolecular Chemistry: Concepts and Perspectives*; VHC: Weinheim, 1995.

(3) Israelachvili, J. *Intermolecular & Surface Forces*, 2nd ed.; Academic Press: London, 1992; Part III.

(4) (a) Merger, F. M.; Litttau, C. A. *J. Am. Chem. Soc*. **1991**, *113*, 1451. (b) Zana, R.; Benrraou, M.; Rueff, R. *Langmuir* **1991**, *11*, 1072. (c) Zana, R.; Talmon, Y. *Nature* **1993**, *362*, 228.

(5) Danino, D.; Talmon, Y.; Zana, R. *Langmuir* **1995**, *11*, 1448.

(6) (a) Bühler, E.; Mendes, E.; Boltnhagen, P.; Munch, J. P.; Zana, R.; Candau, S. J. *Langmuir* **1997**, *13*, 3096. (b) Knaebel, A.; Oda, R.; Mendes, E.; Cadau, S. J. *Langmuir* **2000**, *16*, 2489.

(7) (a) Bhattacharya, S.; De, S. *Chem. Commum*. **1995**, 651. (b) Bhattacharya, S.; De, S. *Langmuir* **1999**, *15*, 3400.

(8) Hait, S. K.; Moulik, S. P. *Curr. Sci*. **2002**, *82*, 1101.

(9) (a) Oda, R.; Huc, I.; Candau, S. J. *Angew. Chem., Int. Ed.* **1998**, *37*, 2689. (b) Oda, R.; Huc, I.; Schmutz, M.; Candau, S. J.; MacKintosh, F. C. *Nature* **1999**, *399*, 566.

(10) (a) Antonietti, M.; Henze, H. P. *Adv. Mater*. **1996**, *8*, 840. (b) Antonietti, M.; Goltner, C.; Henze, H. P. *Langmuir* **1998**, *14*, 2670.

(11) (a) Ulman, A. *An Introduction to Ultrathin Orgaic Films*; Academic: New York, 1991. (b) Ulman, A. *Chem. Rev*. **1996**, *96*, 1533.

(12) (a) Nuzzo, R. G.; Dubois, L. H.; Allara, D. L. *J. Am. Chem. Soc*. **1990**, *112*, 558. (b) Chidsey, C. E. D.; Loiacono, D. N. *Langmuir* **1990**, *6*, 682. (c) Smith, E. L.; Alves, C. A.; Anderegg, J. W.; Porter, M. D.; Siperko, L. M. *Langmuir* **1992**, *8*, 2707. (d) Mukae, F.; Takemura H.; Takehara, K. *Bull. Chem. Soc. Jpn.* **1996**, *69*, 2461.

(13) Tien, J.; Terfort, A.; Whitesides, G. M. *Langmuir* **1997**, *13*, 5349.

(14) Holmlin, R. E.; Chen, X.; Chapman, R. G.; Takayama, S.; Whitesides, G. M. *Langmuir* **2001**, *17*, 2841.

(15) Yuge, R.; Miyazaki, A.; Enoki, T.; Tamada, K.; Nakamura, F.; Hara, M. *J. Phys. Chem. B* **2002**, *106*, 6894.

(16) Regen, S. L.; Samuel, N. K. P.; Khurana, J. M. *J. Am. Chem. Soc*. **1985**, *107*, 5804.

(17) Knoll, W. *Annu. Rev. Phys. Chem*. **1998**, *49*, 569.

(18) Kretschmann, E.; Raether, H. *Z. Naturforsch. Teil* **1968**, *23*, 2135. Raether, H. In *Physics of Thin Films*; Hass, G., Francombe, M. H., Hoffmann, R. W., Eds.; Academic: New York, 1977; Vol. 9, p 145.

(19) Aust, E. F.; Ito, S.; Sawodny, M.; Knoll, W. *Trends Polym. Sci*. **1994**, *9*, 313.

(20) Raether, H. *Surface Plasmons in Smooth and Rough Surfaces and on Gratings*, Springer Tracts in Modern Physics; Springer: Berlin, 1988; Vol. 111.

(21) Tamada, K.; Ishida, T.; Knoll, W.; Fukushima, H.; Colorado, R., Jr.; Graupe, M.; Shmakova, O. E.; Lee, T. R. *Langmuir* **2001**, *17*, 1913.

(22) Poter, M. D.; Bright, T. B.; Allara, D. L.; Chidsedy, C. E. D. *J. Am. Chem. Soc*. **1987**, *109*, 3561.

(23) (a) Walczak, M. M.; Alves, C. A.; Lamp, B. D.; Porter, M. D. *J. Electroanal. Chem*. **1995**, *396*, 103. (b) Castner, D. G.; Hinds, K.; Grainger, D. W. *Langmuir* **1996**, *12*, 5083.

(24) Peterlinz, K. A.; Georgiadis, R. *Langmuir* **1996**, *12*, 4731.

(25) Hostetler, M. J.; Strokes, J. J.; Murray, R. W. *Langmuir* **1996**, *12*, 3604.

(26) L-tartaric acid tends to adsorb more when the density of the SAM is low (ca. 3 h immersed films), suggesting the adsorption of L-tartaric acids on the defect sites.

(27) Because the concentration varied in the SPR cell during the injection of sample solution (during the replacement of absolute solvent to the sample solution), the detailed argument for the kinetics profiles is not appropriate in our experimental system; however, clear change of adsorption rate (e.g., the time to reach a certain surface coverage) was confirmed according to the concentration of original solution.

(28) *Handbook of Data on Organic Compounds*, 2nd edition; CRC press, Inc., 1989.

(29) Bhattacharjee, R.; Jain, Y. S.; Bist, H. D. *J. Raman Spectrosc*. **1989**, *20*, 91.

(30) Lorenzo, M. O.; Haq, S.; Bertrams, T.; Murray, P.; Raval, R.; Baddeley, C. J. *J. Phys. Chem. B* **1999**, *103*, 10661.

(31) Humblot, V.; Haq, S.; Muryn, C.; Hofer, W. A.; Raval, R. *J. Am. Chem. Soc*. **2002**, *124*, 503.

(32) Horvath, J. D.; Gellman, A. J. *J. Am. Chem. Soc*. **2002**, *124*, 2384.